Neutrino- and antineutrino-deuteron elastic scattering and the axial isoscalar nucleon current

T. Frederico,* E. M. Henley, S. J. Pollock, and S. Ying
Department of Physics, FM-15 and Institute for Nuclear Theory, HN-12, University of Washington, Seattle, Washington 98195
(Received 28 October 1991)

We calculate the neutrino and antineutrino elastic scattering cross section on unpolarized deuterons at energies from a few MeV to several GeV and squared momentum transfers up to 5 GeV^2. These cross sections can be used to deduce the unknown weak SU(2) isoscalar and SU(3) flavor-scalar axial-vector coupling to nucleons. This observable can be related to the strangeness axial-vector matrix element in the absence of QCD radiative or isospin-violating corrections. We show that the unknown weak magnetic vector coupling may also be gleaned from these measurements. We use different techniques at different energies, including light-cone impulse approximation at the highest energies, and show that they connect smoothly to each other.

PACS number(s): 25.30.Pt, 24.80.−x, 14.20.Dh, 12.15.Mn

I. INTRODUCTION

The puzzling results of measurements of the πN Σ term [1] and of the proton spin structure function g_1 by the EMC group [2] have suggested that our understanding of the nucleon's structure is far from complete. For instance, the feature that the up (u) and down (d) valence quarks carry the spin of the proton is called into question. Also, the notion that the sea quarks carry none of the spin may well not be correct. In addition, despite numerous theoretical arguments to the contrary [3,4], it is not ruled out that strange quarks play a much larger role in the structure of the nucleon than is generally accepted. For instance, a straightforward explanation of the πN Σ term and g_1 measurements is that there is an appreciable ($\sim 20\%$) probability of strange quarks being in the proton and also contributing to its spin [5,6]. Since one may think of the proton "dissociating" into a $\Lambda(\Sigma)$ and K, it is not surprising that some strange-quark presence should be expected.

If strange quarks do contribute to the nucleon structure functions, then they give rise to new weak form factors and alter other ones. If only up and down quarks are present, then the weak nucleon form factors at zero momentum transfer $F_i(0)$ for the weak vector and axial-vector currents

$$\begin{aligned}\langle N|J_\mu|N\rangle &= \bar{U}(p')\frac{1}{2}\left[(F_1^{\rm IS}+F_1^{\rm IV}\tau_3)\gamma_\mu \right.\\ &\left. +i\sigma_{\mu\nu}\frac{q^\nu}{2m}(F_2^{\rm IS}+F_2^{\rm IV}\tau_3)\right]U(p)\ ,\\ \langle N|J_\mu^{(5)}|N\rangle &= \bar{U}(p')\frac{1}{2}\left[(F_A^{\rm IS}+F_A^{\rm IV}\tau_3)\gamma_\mu\gamma_5 \right.\\ &\left. +(F_P^{\rm IS}+F_P^{\rm IV}\tau_3)\frac{q_\mu}{m_\mu}\gamma_5\right]U(p)\end{aligned} \quad (1)$$

are determined by conserved vector current (CVC), partially conserved axial-vector current, and the neutron β decay. In Eq. (1) q is the momentum transfer, m is the nucleon mass, U is the nucleon spinor, and IS and IV are the isoscalar and isovector components, respectively.

In the standard model with only u and d quarks, we have

$$\begin{aligned}&F_1^{\rm IS}(0)=-2\sin^2\theta_W,\quad F_1^{\rm IV}=(1-2\sin^2\theta_W)\ ,\\ &F_2^{\rm IS}(0)=-2\kappa_S\sin^2\theta_W,\quad F_2^{\rm IV}=\kappa_V(1-2\sin^2\theta_W)\ ,\\ &F_A^{\rm IS}(0)=0,\quad F_A^{\rm IV}(0)=g_A=-1.26\ ,\end{aligned} \quad (2)$$

where the superscripts refer to isospin, $\sin^2\theta_W\approx 0.23$ with θ_W the weak mixing angle, $\kappa_S\approx -0.12$ is the isoscalar anomalous magnetic moment, and $\kappa_V\approx 3.7$ is the isovector anomalous magnetic moment. F_P is the induced pseudoscalar coupling, which does not contribute to neutrino scattering.

If strange quarks contribute to the nucleon's structure, they may modify the normalization and four-momentum dependence of the weak form factors. Although $F_1(0)$ is still fixed by $\sin^2\theta_W$ (since the net strangeness of the proton is constrained to zero), the momentum dependence of $F_1^{\rm IS}$ and $F_1^{\rm IV}$ is no longer determined from the electromagnetic form factors by CVC. There could also be new magnetic and axial contributions, even at $q^2=0$, denoted by F_2^s and F_A^s (defined below) where s stands for strange. These new contributions allow tests for the presence of strangeness matrix elements in the nucleon to be carried out [7–9]. Among these tests is a determination of $F_A^{\rm IS}=-F_A^s$ (see below), which we examine in detail, via the ratio

$$R=\frac{d\sigma(\nu d\to\nu d)-d\sigma(\bar{\nu}d\to\bar{\nu}d)}{d\sigma(\nu d\to\nu d)+d\sigma(\bar{\nu}d\to\bar{\nu}d)}\ . \quad (3)$$

This ratio vanishes in the absence of an isoscalar axial-vector matrix element. In the presence of strangeness, it is advantageous to use an SU(3) notation; however, we do not assume SU(3) symmetry. We define the underlying weak and electromagnetic current operators by [9]

*Permanent address: Instituto de Estudos Avançados, Centro Técnico Aeroespacial, 12.225 São José dos Campos, São Paulo, Brazil.

$$J_\mu^\gamma = \tfrac{2}{3}\bar{u}\gamma_\mu u - \tfrac{1}{3}\bar{d}\gamma_\mu d - \tfrac{1}{3}\bar{s}\gamma_\mu s + \cdots$$
$$= \sum_{\alpha=0,3,8} \bar{q}\gamma_\mu a^\alpha \lambda^\alpha q \ , \tag{4a}$$
$$J_\mu^{\text{weak}} = \tfrac{1}{2}\bar{u}\gamma_\mu(1-\gamma^5)u - \tfrac{1}{2}\bar{d}\gamma_\mu(1-\gamma_5)d$$
$$-\tfrac{1}{2}\bar{s}\gamma_\mu(1-\gamma_5)s - 2\sin^2\theta_W J_\mu^\gamma$$
$$= \sum_{\alpha=0,3,8} \bar{q}\gamma_\mu[2b^\alpha(1-\gamma^5) - 2\sin^2\theta_W a^\alpha]\lambda^\alpha q \ , \tag{4b}$$

where q is the (current) quark field operator, λ^α are the Gell-Mann SU(3) matrices, normalized to $\mathrm{Tr}(\lambda^a\lambda^b)=\delta^{ab}/2, \lambda^0=\frac{1}{3}\mathbf{1}$, and for the proton

$$a^0=0, \quad b^0=-\tfrac{1}{4} \ ,$$
$$a^3=+1, \quad b^3=+\tfrac{1}{2} \ , \tag{4c}$$
$$a^8=1/\sqrt{3}, \quad b^8=+1/(2\sqrt{3}) \ .$$

The matrix elements with nucleon states yield $(i=1,2,A,P)$

$$F_i^0 = \tfrac{1}{3}(F_i^\mu + F_i^d + F_i^s) \ ,$$
$$F_i^3 = \tfrac{1}{2}(F_i^u - F_i^d) \ , \tag{5}$$
$$F_i^8 = (1/2\sqrt{3})(F_i^u + F_i^d - 2F_i^s) \ ,$$

where these quark form factors are defined in exact analogy with Eq. (1); as an example, we have

$$\langle p'|\bar{s}\gamma_\mu s|p\rangle \equiv \bar{U}(p')\left[F_1^s(q^2)\gamma_\mu + \frac{i\sigma_{\mu\nu}q^\nu}{2m}F_2^s(q^2)\right]U(p) \ .$$

Finally, the full weak nucleon form factors are thus given by

$$F_{1,2} = \sum_{\alpha=0,3,8} 2(b^\alpha - a^\alpha \sin^2\theta_W)F_{1,2}^\alpha$$
$$= \sum_{j=u,d,s} (\tfrac{1}{2}\tau_j^{(3)} - 2Q_j\sin^2\theta_W)F_{1,2}^j \ , \tag{6}$$
$$F_{A,P} = \sum_{\alpha=0,3,8} -2b^\alpha F_{A,P}^\alpha$$
$$= \sum_{j=u,d,s} -\tfrac{1}{2}\tau_j^{(3)}F_{A,P}^j \ , \tag{7}$$

with $\tau_j^{(3)}$ the third component of the weak isospin Pauli matrix ($\tau^{(3)}=1$ for left-handed u quarks; $\tau^{(3)}=-1$ for left-handed d and s quarks). Since $F^{\text{IS}}\equiv F^p+F^n$, and SU(2) symmetry on the nucleon gives

$$(F_i^{0,8})^p = (F_i^{0,8})^n \ ,$$
$$(F_i^3)^p = -(F_i^3)^n \ , \tag{8}$$

it follows that

$$F_A^{\text{IS}} = -F_A^s \ . \tag{9}$$

For the matrix elements of the nucleon, we have introduced the form factors $F_i^{(0)}, F_i^{(3)}, F_i^{(8)}$, corresponding to the SU(3) matrices $\lambda^{(0)}, \lambda^{(3)}$, and $\lambda^{(8)}$.

In a previous publication [8], we have used an impulse approximation and a single-deuteron form factor [valid for squared momentum transfers $q^2=-Q^2 \gtrsim -0.5$ $(\text{GeV}/c)^2$] to evaluate R. In this paper, we go beyond this approximation and consider three regions of energy: (A) $E_\nu \lesssim 150$ MeV, (B) $E_\nu \lesssim 1$ GeV, and (C) $E_\nu \lesssim 5$ GeV. These regions overlap, but we have used different calculational techniques for the various energy regions. In all cases, we use an impulse approximation and neglect off-mass-shell effects and the small ($\lesssim 1\%$) isospin violation. In region A we use a nonrelativistic reduction of the current operators in Eq. (1), together with a multipole decomposition [10] and some meson exchange effects, through the use of an extended Siegert theorem to evaluate the matrix elements for a deuterium target in the laboratory frame [11]. In region B we use a covariant formalism together with a nonrelativistic deuteron wave function in the Breit frame [12]. Meson exchange currents are neglected since they are predominantly due to the pion of isospin 1, which does not contribute to elastic scattering in lowest order. In region C we use a light-cone impulse approximation [13], which projects an instant-form nonrelativistic deuteron wave function onto the light cone, and boosts it to the Breit frame. Although exchange currents are also neglected, the light-cone technique has been shown to include some two-body effects [14]. As we will show, there is a smooth transition from one region to the next one.

II. THEORY

A. Low-energy region: $Q^2 \lesssim (400\ \text{MeV}/c)^2$

The elastic neutrino scattering from deuterium is mediated solely by neutral currents (unless very small multiple scattering effects are considered). The differential cross section can be written as

$$d\sigma = \frac{2\pi}{2E_\nu}\tfrac{1}{3}\,\mathrm{Tr}[H_w H_w^\dagger]\delta(E_\nu + E_d - E'_\nu - E'_d)d\xi \ , \tag{10}$$

where E_ν and E'_ν are the initial and final neutrino energies, E_d, E'_d are those of the deuteron, Tr is a trace over spin degrees of freedom, H_w is the weak Hamiltonian, and $d\xi$ is the phase-space element

$$d\xi = \frac{d^3k'_\nu}{2E'_\nu(2\pi)^3} \ . \tag{11}$$

We express the cross section in terms of the squared momentum transfer $q^2=-Q^2$; the transformation is

$$\frac{d\sigma}{dQ^2} = \frac{d\sigma}{d\Omega_\nu}\frac{\pi}{E'^2_\nu} \ . \tag{12}$$

For unpolarized initial and final states, we have

$$\tfrac{1}{3}\,\mathrm{Tr}[H_w H_w^\dagger] = \tfrac{1}{6}G_F^2\,\mathrm{Tr}[J_\mu^\dagger(-q)J_\nu(-q)]\,\mathrm{Tr}[l^\mu(q)l^{\nu\dagger}(q)] \ , \tag{13}$$

where J_μ and l^μ are the nucleon and lepton currents, and G_F is the Fermi weak coupling constant. The leptonic trace is

$$L^{\mu\nu} = \frac{2}{E_\nu E'_\nu}(k^\mu k'^\nu + k^\nu k'^\mu - g^{\mu\nu}k\cdot k' \mp i\epsilon^{\mu\nu\alpha\beta}k'_\alpha k_\beta) \ ,$$

where the upper sign holds for ν's and the lower one for $\bar{\nu}$'s. In region A we have

$$\frac{d\sigma}{d\Omega_\nu}=\frac{\gamma}{3\pi}G_F^2E'_\nu k'_\nu(R_a\pm R_b)\ ,$$

$$\gamma=\frac{1}{1+(E'_\nu-E_\nu\cos\theta)/E_d}\ , \tag{14}$$

where M is the mass of the deuteron, and the response functions R_a and R_b can be related to a set of irreducible hadronic response functions $R_{ss}\cdots R_{vv}$ of rank zero (defined in the Appendix) through

$$R_{a,\nu}^{(0)}=3\left[\frac{1}{\sqrt{3}}R_{ss}(0)L_{ss}-\frac{1}{\sqrt{3}}R_{sv}^{+}(01)\hat{\mathbf{q}}\cdot\mathbf{L}_{sv}^{+}+\frac{1}{\sqrt{3}}R_{vv}(000)L_{vv}^{0}+\frac{1}{\sqrt{2}}R_{vv}(022)T_2(\hat{\mathbf{q}}):\mathbf{L}_{vv}^{2}\right], \tag{15}$$

$$R_{b,\nu}^{(0)}=-\sqrt{3}R_{vv}(011)\hat{\mathbf{q}}\cdot\mathbf{L}_{vv}^{1}\ , \tag{16}$$

with $T_2^{ij}(\hat{\mathbf{q}})=\hat{q}^i\hat{q}^j-\frac{1}{3}\delta^{ij}$, $T_2(\hat{\mathbf{q}}):\mathbf{ab}=T_2^{ij}(\hat{\mathbf{q}})a_ib_j$, and leptonic kinematical functions

$$L_{ss}=1+\hat{\mathbf{k}}'_\nu\cdot\hat{\mathbf{k}}_\nu\ , \tag{17}$$

$$\mathbf{L}_{sv}^{+}=\hat{\mathbf{k}}_\nu+\hat{\mathbf{k}}'_\nu\ , \tag{18}$$

$$L_{vv}^{0}=-\sqrt{3}(1-\tfrac{1}{3}\hat{\mathbf{k}}'_\nu\cdot\hat{\mathbf{k}}_\nu)\ , \tag{19}$$

$$L_{vv}^{1}=\sqrt{2}(\hat{\mathbf{k}}'_\nu-\hat{\mathbf{k}}_\nu)\ , \tag{20}$$

$$\mathbf{L}_{vv}^{2}=2\hat{\mathbf{k}}'_\nu\hat{\mathbf{k}}_\nu\ . \tag{21}$$

The set of universal hadronic response functions is evaluated with a nonrelativistic deuteron wave function in the laboratory frame of reference. They can be expanded in terms of bilinear products of the reduced matrix elements of the multipole operators of the hadronic weak current operators. The resulting expressions are

$$R_{a,\nu}^{(0)}=\sum_{\lambda J_f J}\left[|C_J(\lambda J_f)|^2L_{ss}+2\,\mathrm{Re}C_J(\lambda J_f)\mathcal{L}_J^*(\lambda J_f)\hat{\mathbf{q}}\cdot\mathbf{L}_{sv}^{+}+|\mathcal{L}_J(\lambda J_f)|^2\times\left[T_2(\hat{\mathbf{q}}):\mathbf{L}_{vv}^{2}-\frac{1}{\sqrt{3}}L_{vv}^{0}\right]+[|\mathcal{E}_J(\lambda J_f)|^2+|\mathcal{M}_J(\lambda J_f)|^2]\left[\frac{1}{2}T_2(\hat{\mathbf{q}}):\mathbf{L}_{vv}^{2}+\frac{1}{\sqrt{3}}L_{vv}^{0}\right]\right], \tag{22}$$

$$R_{b,\nu}^{(0)}=\sqrt{2}\sum_{\lambda J_f J}\mathrm{Re}\mathcal{E}_J(\lambda J_f)\mathcal{M}_J^*(\lambda J_f)\hat{\mathbf{q}}\cdot\mathbf{L}_{vv}^{1}\ . \tag{23}$$

In terms of the response function for the deuteron of spin 1, the ratio R is given by

$$R=R_b/R_a\ , \tag{24}$$

with

$$R_b=\sqrt{2}\,\mathrm{Re}(E_1^5M_1^*+E_2M_2^{5*})\hat{\mathbf{q}}\cdot\mathbf{L}_{vv}^{1}\ , \tag{25}$$

$$R_a=\left[(|C_0|^2+|C_1^5|^2+|C_2|^2)L_{ss}+(|L_0|^2+|L_1^5|^2+|L_2|^2)\left[T_2(\hat{\mathbf{q}}):\mathbf{L}_{vv}^{2}-\frac{1}{\sqrt{3}}L_{vv}^{0}\right]+2\,\mathrm{Re}(C_0L_0^*+C_1^5L_1^{5*}+C_2L_2^*)\hat{\mathbf{q}}\cdot\mathbf{L}_{sv}^{+}-(|M_1|^2+|E_1^5|^2+|E_2|^2)\left[\frac{1}{2}T_2(\hat{\mathbf{q}}):\mathbf{L}_{vv}^{2}+\frac{1}{\sqrt{3}}L_{vv}^{0}\right]\right]. \tag{26}$$

B. Intermediate-energy region

For energies above $\sim$100 MeV we have used a covariant formulation for the scattering [12], albeit we keep a nonrelativistic deuteron wave function to evaluate body form factors in the Breit frame. In this approach, also sometimes called an "elementary particle treatment" [15], one makes use of deuteron elastic form factors. Nonrelativistic, one-body current operators and wave functions are then used to provide a (model-dependent) approximation to these covariant form factors. This formalism is described in some detail in Refs. [12] and [15], and references therein. We begin with elastic deuteron matrix elements of weak currents written as [15–17]

$$\langle D'|J_\mu|D\rangle\equiv\frac{-1}{\sqrt{4D_0D'_0}}\left[G_1(Q^2)(\xi'^*\cdot\xi)P_\mu+G_2(Q^2)[\xi_\mu(\xi'^*\cdot q)-\xi'^*_\mu(\xi\cdot q)]-G_3(Q^2)(\xi\cdot q)(\xi'^*\cdot q)\frac{P_\mu}{2M^2}\right], \tag{27}$$

$$\langle D'|J_\mu^{(5)}|D\rangle\equiv\frac{-1}{\sqrt{4D_0D'_0}}\left[iG_4(Q^2)\epsilon_{\mu\alpha\beta\gamma}\xi'^{*\alpha}\xi^\beta P^\gamma+\frac{iG_5(Q^2)}{M^2}\epsilon_{\mu\alpha\beta\gamma}q^\alpha P^\beta[\xi^\gamma(\xi'^*\cdot q)-\xi'^{\gamma*}(\xi\cdot q)]\right], \tag{28}$$

where $P^\mu=p_d'^\mu+p_d^\mu$, p_d (p_d') is the deuteron's initial (final) momentum, $D_0=\sqrt{M^2+Q^2/4}$ is the deuteron energy in the Breit frame, and ξ_μ (ξ'_μ) is the polarization four-vector for the initial (final) deuteron. In writing (27) and (28), we have already assumed vector current conservation, time-reversal symmetry, Hermiticity, and the absence of second-class currents. It is also common, and convenient, to rewrite the three-vector terms into linear

combinations corresponding to charge, quadrupole, and magnetic form factors:

$$G_C(Q^2)\equiv G_1(Q^2)-(Q^2/6M^2)G_Q(Q^2)\ ,$$
$$G_Q(Q^2)\equiv G_1(Q^2)-G_2(Q^2)+(1-Q^2/4M^2)G_3(Q^2)\ ,$$
$$G_M(Q^2)\equiv G_2(Q^2)\ . \tag{29}$$

The neutrino-deuteron elastic cross sections are then given by

$$\frac{d\sigma_{\nu(\bar{\nu})d}}{d\Omega}=\frac{G_F^2E_\nu'^2}{2\pi^2}r\left[2\sin^2\frac{\theta}{2}W_1+\cos^2\frac{\theta}{2}W_2 \mp\frac{2}{M}(E_\nu+E_\nu')\sin^2\frac{\theta}{2}W_8\right], \tag{30}$$

with θ the lepton scattering angle in the laboratory frame and E_ν (E_ν') the initial (final) neutrino energy. The nuclear recoil factor $r=[1+(1-\cos\theta)E_\nu/M]^{-1}$, and the response functions are given by

$$W_1(q^2)=\frac{Q^2}{6M^2}\left[1+\frac{Q^2}{4M^2}\right]G_M^2+\frac{2}{3}\left[1+\frac{Q^2}{4M^2}\right]^2G_A^2\ ,$$
$$W_2(q^2)=\left[G_C^2+\frac{Q^2}{6M^2}G_M^2+\frac{Q^4}{18M^4}G_Q^2+\frac{2}{3}\left[1+\frac{Q^2}{4M^2}\right]G_A^2\right], \tag{31}$$
$$W_8(q^2)=\frac{2}{3}\left[1+\frac{Q^2}{4M^2}\right][G_MG_A]\ ,$$

with $G_A\equiv G_4+(Q^2/M^2)G_5$. The relation of $d\sigma/dQ^2$ to $d\sigma/d\Omega$ is found immediately from $d\Omega/dQ^2=\pi/E_\nu'^2$.

Equation (31) involves no deuteron-model-dependent approximations. In order to explicitly evaluate and compute the body form factors G_1-G_5, we recast Eqs. (27) and (28) in the Breit frame into a nonrelativistic appearance [16]. The left-hand sides are explicitly evaluated using nonrelativistic reduced single-nucleon current operators in the Breit frame for the deuteron [10]:

$$J_0=F_E(Q^2),\quad J_0^{(5)}=\frac{F_A(q^2)}{2m}\sigma\cdot(\mathbf{p}+\mathbf{p}')=0\ ,$$
$$\mathbf{J}=\left[F_M(Q^2)\frac{i}{2m}\sigma\times\mathbf{q}+\frac{F_E(q^2)}{2m}(\mathbf{p}+\mathbf{p}')\right], \tag{32}$$
$$\mathbf{J}^{(5)}=F_A(Q^2)\sigma\ ,$$

where the $F_{E,M}$'s are the free, single-nucleon (electric, magnetic) Sachs form factors, which are related to F_1 and F_2 in the usual manner.

Furthermore, we use S- and D-state deuteron wave functions $u(r)$ and $w(r)$, as given by various popular nonrelativistic potential models [18]. After some algebra, we compare the derived expressions for the matrix elements with the general form for the right side in the Breit frame, yielding the usual expressions for $G_{C,Q,M}$ [12,16] and for the axial piece

$$G_A=F_A(q^2)\frac{M}{D_0}\int_0^\infty\left[u^2-\frac{w^2}{2}\right]j_0\left[\frac{qr}{2}\right]+\frac{(w^2+\sqrt{2}uw)}{2}j_2\left[\frac{qr}{2}\right]dr\ , \tag{33}$$

where the j's are spherical Bessel functions, $q\equiv\sqrt{Q^2}$, and $F_{E,M,A}\equiv F_{E,M,A}^p+F_{E,M,A}^n$ are the weak isoscalar nucleon elastic form factors.

A strange-quark presence in the deuteron is included at this level by simply allowing s-quark contributions to the isoscalar nucleon form factors. From Eqs. (2) and (4), and assuming only good SU(2) symmetry at the nucleon level, we can relate weak, electromagnetic, and strange nucleon form factors. For the proton, we have for the weak electric, magnetic, and axial form factors

$$F_{E,M}^p=(\tfrac{1}{2}-2\sin^2\theta_W)F_{E,M}^{\gamma,p}-\tfrac{1}{2}(F_{E,M}^{\gamma,n}+F_{E,M}^s)\ ,$$
$$F_A^p=\tfrac{1}{2}F_A^{cc,p}-\tfrac{1}{2}F_A^s\ . \tag{34}$$

with cc indicating the charge-changing (isovector) axial form factor. None of the strange-quark form factors appearing above are firmly established experimentally, and we use arbitrary parametrizations in our calculations to look for experimental sensitivities to them. (To minimize the number of unknown parameters, we assume the usual dipole forms for the Q^2 dependence.) We can now immediately compute the neutrino-deuteron elastic cross sections of interest from Eqs. (30), (31), (33), and (34).

C. High-energy region

For still higher energies and momentum transfers, we use light-front dynamics. This method was developed in Refs. [14] and [19].

In light-front dynamics, the form factors of the vector and axial-vector currents of the deuteron are calculated from the + component of the currents. The null plane is defined by $x^+=x^0+x^3=0$. The construction of the + component of the currents in the light front also uses nonrelativistic deuteron wave functions [10]. Due to the cluster separability property of the square of the free mass operator for two particles [21], the c.m. (center-of-mass) coordinate can be separated. The free mass operator of the two-body system is expressed by means of the null-plane momenta. The third component of the relative momentum can be defined as a function of the relative perpendicular momentum and the variable $\xi=p^+/p_d^+$, which is analogous to the nonrelativistic mass; p^+ ($=p^0+p^3$) is the nucleon light-front momentum and p_d^+ is the same quantity for the deuteron momentum.

The coupling of the angular momentum and spin is also carried out in the c.m. frame, but in the instant form, and reexpressed in terms of light-cone spinors; this gives the front form of the Clebsch-Gordan coefficients [14,19,20]. The deuteron is boosted like the two single-nucleon light-cone wave functions, in contrast to the usu-

al technique of employing the boost operator in the instant form. The null-plane impulse approximation means that one is projecting the instant form of the wave function onto the light cone and then boosting it to the Breit frame.

The matrix elements of the deuteron currents are calculated in the Breit frame where the momentum transfer is chosen such that $q^+=0$ and $\mathbf{q}_\perp=(q_x,0,0)$; with this choice the current is conserved when we calculate J^+. The matrix element of the vector and axial-vector ($J^{(5)+}$) currents in the deuteron light-cone basis come from the integrals [13,19]

$$(n',\mathbf{q}_\perp/2|J^{\mathrm{IS}+}|n,-\mathbf{q}_\perp/2) = \int d\xi\, d\mathbf{k}_\perp \Phi_d^\dagger(\xi,\mathbf{k}'_\perp,n')(p'|J^{\mathrm{IS}+}|p)\Phi_d(\xi,\mathbf{k}_\perp,n) , \tag{35a}$$

$$(n',q_\perp/2|J^{\mathrm{IS}(5)+}|n,-q_\perp/2) = \int d\xi\, dk_\perp \Phi_d^\dagger(\xi,\mathbf{k}'_\perp,n')(p'|J^{\mathrm{IS}(5)+}|p)\Phi_d(\xi,\mathbf{k}_\perp,n) , \tag{35b}$$

where the matrix element of the isoscalar vector (axial) nucleon current $J^{\mathrm{IS}+}$ ($J^{\mathrm{IS}(5)+}$) is calculated with the light-cone spinors [21]; $\mathbf{k}'_\perp=\mathbf{k}_\perp+(1-\xi)\mathbf{q}_\perp$, and n' and n are the deuteron spin projections. In the above expressions the wave functions in the rounded bras and kets are on the light cone. The deuteron wave function in the null plane is connected to the equal time one by a Melosh rotation of the spins in the c.m. [19–21]:

$$\Phi_d(\xi,\mathbf{k}_\perp)=R_M^\dagger(\xi,\mathbf{k}_\perp)R_M^\dagger(1-\xi,-\mathbf{k}_\perp) \times\frac{\phi_d(\mathbf{k})}{\sqrt{\xi}}\frac{(\mathbf{k}_\perp^2+m^2)^{1/4}}{2[\xi(1-\xi)]^{3/4}} , \tag{36}$$

where

$$k_z=(\xi-\tfrac{1}{2})\left[\frac{\mathbf{k}_\perp^2+m^2}{\xi(1-\xi)}\right]^{1/2} \tag{37}$$

is the third component of $\mathbf{k}$, the relative momentum [14]. The normalization factor in the definition of the null-phase deuteron wave function in Eq. (36) arises from the Jacobian of the transformation [19] of $k_z,\mathbf{k}_\perp\to\xi,\mathbf{k}_\perp$, and a factor of $\xi^{-1/2}$ appears to take into account the normalization of the current J^+ at zero momentum transfer. The matrix element of the nucleon isoscalar vector current J^{IS} at $q^+=0$ is

$$(p'|J^{\mathrm{IS}+}|p)=\frac{p_d^+\xi}{m_n}\left[F_1^{\mathrm{IS}}-i\frac{F_2^{\mathrm{IS}}}{2M}(\mathbf{q}_\perp\times\boldsymbol{\sigma})_z\right] . \tag{38}$$

The deuteron vector current $J^{\mathrm{IS}+}$ in the light-cone basis can be obtained by applying a Melosh rotation to the instant-form representation [22], and in the Breit frame it becomes

$$J^{\mathrm{IS}+}=\frac{G_C}{1+\eta}\begin{bmatrix}1&\sqrt{2\eta}&\eta\\-\sqrt{2\eta}&1-\eta&\sqrt{2\eta}\\\eta&-\sqrt{2\eta}&1\end{bmatrix} +\frac{G_Q\eta}{3(1+\eta)}\begin{bmatrix}1&\sqrt{2}\eta&-3-2\eta\\-\sqrt{2\eta}&-2+4\eta&\sqrt{2\eta}\\-3-2\eta&-\sqrt{2\eta}&1\end{bmatrix} +\frac{G_M\sqrt{2\eta}}{2(1+\eta)}\begin{bmatrix}\sqrt{2\eta}&\eta-1&-\sqrt{2\eta}\\1-\eta&2\sqrt{2\eta}&\eta-1\\-\sqrt{2\eta}&1-\eta&\sqrt{2\eta}\end{bmatrix} , \tag{39}$$

where $\eta=Q^2/4M^2$.

From the rotational properties of the deuteron wave function, it appears that there are four independent matrix elements in the null-plane impulse approximation; they are $(J^+_{11},J^+_{10},J^+_{1-1},J^+_{00})$. From Eq. (39) it can be seen that these matrix elements are not independent; the following angular condition holds [19,20]:

$$J^+_{10}=\frac{\sqrt{2\eta}}{2}J^+_{11}-\frac{1}{2\sqrt{2\eta}}(J^+_{00}-J^+_{11}-J^+_{1-1}) . \tag{40}$$

The matrix elements of J^+ calculated from Eq. (35a) violate the angular condition, and this fact gives rise to different prescriptions for the magnetic deuteron form factor at large q^2 in Refs. [19] and [23]. According to Ref. [19], the form factors can be written as

$$\begin{aligned}G_C&=h_0+\tfrac{1}{6}h_2-\tfrac{2}{3}\eta(h_0+h_2+\tfrac{5}{2}h_1) ,\\ G_M&=2h_0+h_2+h_1(1-\eta) ,\\ G_Q&=\frac{3\sqrt{2}}{4\eta}[h_2+\eta(\tfrac{1}{2}h_2-h_0-h_1)] ,\end{aligned} \tag{41}$$

where

$$\begin{aligned}h_0&=\frac{1}{2(1+\eta)}(J^+_{11}+J^+_{00}) ,\\ h_1&=-\frac{\sqrt{2}}{\sqrt{\eta}(1+\eta)}J^+_{10} ,\\ h_2&=-\frac{1}{1+\eta}J^+_{1-1} .\end{aligned}$$

In Ref. [23] the form factor G_M is written as

$$G_M=2\left[J^+_{11}-\frac{J^+_{10}}{\sqrt{2\eta}}\right] . \tag{42}$$

The expressions for G_M are equivalent if the angular condition (40) holds, but they do give different results for large momentum transfers. In the particular case of a pure S-wave deuteron this problem disappears [13].

The null-plane matrix element of the nucleon isoscalar axial current which is needed for the impulse approximation is

$$\langle p'|J^{\mathrm{IS}(5)+}|p\rangle=\frac{p_d^+\xi}{m}F_A^{\mathrm{IS}}\sigma_z . \tag{43}$$

The deuteron axial current has three form factors [15], but using parity and time-reversal properties, one is able to show that only two of them are independent; only the

combination proportional to G_A in Eq. (31) is relevant for our calculation. The matrix element of the axial current in the Breit frame and in the instant form is [13]

$$J^{\mathrm{IS}(5)+}_{\mathrm{inst}} = \frac{p_d^0}{M} G_A S_z \ . \tag{44}$$

The null-plane matrix element of $J^{\mathrm{IS}(5)+}$ is obtained from Eq. (44) by applying the Melosh rotation for a spin-1 particle. Then, we have

$$J^{\mathrm{IS}(5)+} = G_A \begin{bmatrix} 1 & \sqrt{\eta/2} & 0 \\ -\sqrt{\eta/2} & 0 & -\sqrt{\eta/2} \\ 0 & \sqrt{\eta/2} & -1 \end{bmatrix} . \tag{45}$$

Due to current conservation for the neutrino, only G_A enters into the calculation of R. The matrix element $J^{(5)+}_{11}$ is used because it gives the usual nonrelativistic limit for G_A [13], although, in principle, the axial form factor of the deuteron can be calculated from $J^{(5)+}_{11}$ or $J^{(5)+}_{10}$.

III. RESULTS AND DISCUSSION

In Fig. 1 we show the calculated differential cross sections for incident ν and $\bar{\nu}$ energies of 500 MeV. The quantity $d\sigma/dQ^2$ is a function of Q^2 (or θ) and E_ν, although it is determined primarily by Q^2. For this figure, as well as in most of our work, we use the Paris potential to bind the deuteron and a dipole fit to the nucleon form factors. The curves shown are for $F_A^s(0)=0.2$ and for the three methods of calculations. Even though the largest momentum transfers possible are higher than those applicable for method A, the agreement with the other two methods is good for $Q^2 \lesssim 0.5$ (GeV/c)^2, which corresponds to backscattering at $E_\nu \gtrsim 400$ MeV. The differential cross sections agree even better at lower neutrino energies. At higher energies, e.g., for $E_\nu \gtrsim 1$ GeV, differences between methods B and C become significant at large Q^2 (see Fig. 5) because the zeros of the deuteron body form factors differ somewhat from each other. At these large values of Q^2, measurements become correspondingly difficult because the elastic differential cross section drops significantly due to the falloff of the deuteron form factors.

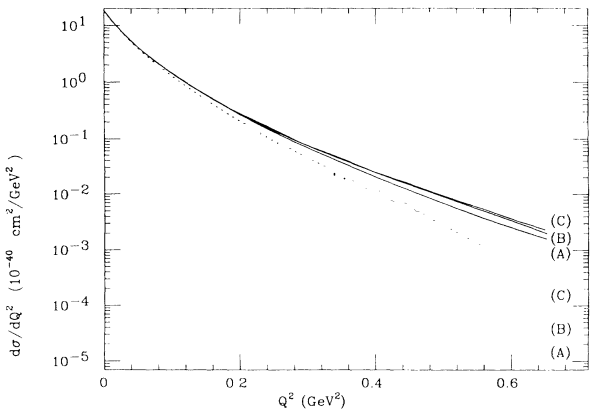

FIG. 1. Neutrino (solid) and antineutrino (dotted) differential cross sections as a function of Q^2 for methods A, B, and C.

The key feature we wish to call attention to is the ratio R [Eq. (3)] of the difference of ν and $\bar{\nu}$ cross sections divided by their sum. The numerator of R is directly proportional to the interference of axial and vector magnetic deuteron form factors. It vanishes identically if there are no axial isoscalar matrix elements since neutrino and antineutrino cross sections would then be identical. It is for this reason that R is a promising observable to study the s-quark spin matrix elements in the nucleon.

Figure 2 shows the ratio R at $E_\nu=250$ MeV. The curves for the different methods agree with each other to better than a few percent at the largest Q^2 and converge smoothly at low Q^2. In Fig. 3 we show R at $E_\nu=500$ MeV for methods B and C, where the agreement is also very good. We have omitted a curve for method A because it is not applicable at the higher Q^2 accessible here. As can be seen from both figures, R grows smoothly and monotonically from 0 to 1 for both $F_A^s(0)=0.1$ and 0.2. Its value is larger than $\frac{1}{4}$ for reasonable values of Q^2, e.g., $Q^2 \gtrsim 0.4$ (GeV/c)^2. The magnitudes of $F_A^s(0)$ represented in these figures are typical of those obtained from Ref. [2] and from measurements of the elastic ν and $\bar{\nu}$ scattering cross sections on H. We assume the Q^2 dependence of the isoscalar axial form factor to be the same as its isovector partner [24].

The sign of R is fixed by the sign of $F_A^s(0)$. From Figs. 2 and 3 one sees that even a fairly conservative value of $F_A^s(0)=0.1$ yields a large ($\sim 100\%$) difference in ν and $\bar{\nu}$ cross sections at large Q^2. At the highest values of Q^2, the ratio R is no longer proportional to F_A^s because the square of this form factor contributes to the denominator. In Figs. 4 and 5, R is shown as a function of Q^2 at $E_\nu=1$ and 2 GeV. At these energies the simple behavior of R present at lower energies is absent. Here, even for a small value of $F_A^s(0)=0.1$, R rises at small angles, but it is forced back down to zero at $Q^2=1.5$ (GeV/c)^2, where the first zero of the deuteron form factor occurs. Both magnetic and axial form factors vanish at roughly the same Q^2; the exact location of these and further zeros is quite model dependent, so that there is considerable variation of R at large Q^2. The variations of R for the Paris

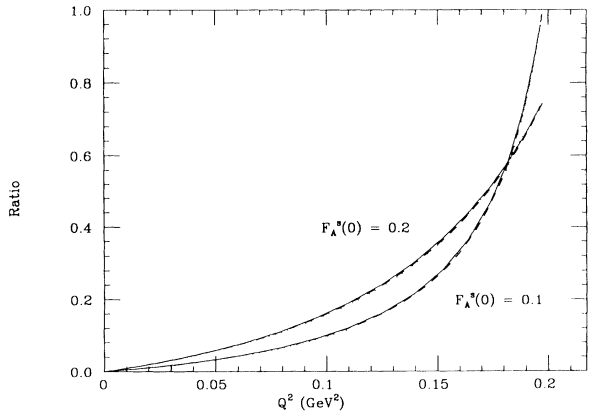

FIG. 2. The ratio R as a function of Q^2 at $E_\nu=250$ MeV for $F_A^s(0)=0.1$ (lower curves at small Q^2) and 0.2 (upper curves at small Q^2) and for methods A (dotted), B (dashed), and C (solid).

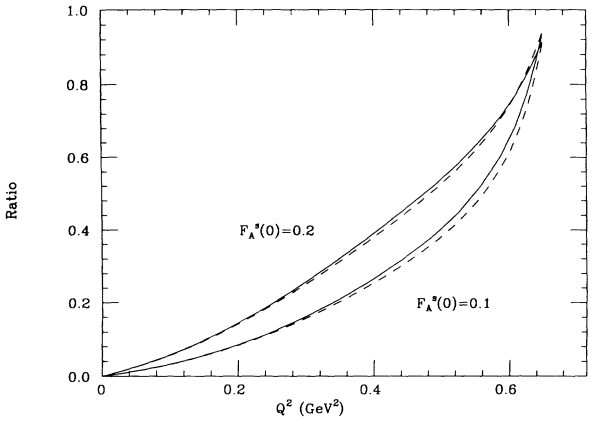

FIG. 3. Same as Fig. 2 at $E_\nu=500$ MeV; only curves for methods B and C are shown.

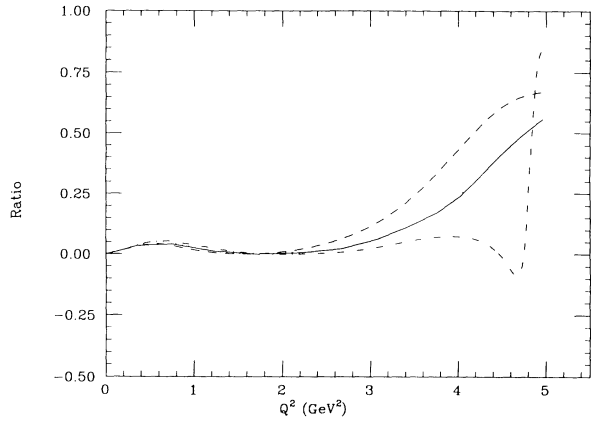

FIG. 5. Same as Fig. 4 at $E_\nu=2$ GeV.

and Bonn potentials [18] appear in both Figs. 4 and 5. The Bonn potential produces a second diffraction minimum in both axial and magnetic form factors for $Q^2\approx 4.5$ (GeV/c)^2, while the Paris potential does not. The second minima for the axial and magnetic form factors are separated, so that R flips sign and grows fairly large before being pulled back to zero. The two calculational techniques B and C differ considerably in their treatment of relativistic corrections, and also yield a quite different behavior of R at these large Q^2. Thus, it is quite clear that, in order to extract a quantitative value of $F_A^s(0)$ or of the deuteron weak form factors more generally, it is necessary to remain at $Q^2<1$ (GeV/c)^2. Since the cross section drops rapidly with Q^2, this constraint is compatible with experimental requirements.

In Fig. 6 we further examine the role of the nucleon-nucleon potential, as well as the role of uncertain nucleon properties, on our calculated quantities; the Gari-Krumpelmann [25] form factors for the nucleon are used as a variant of the dipole ones. The variations produced by the use of Bonn, Reid, and Paris N-N potentials, and the change in form factors, are all included within the uncertainty band shown in Fig. 6; the spread due to the calculational techniques (B or C) are no longer than this error band.

We next examine the sensitivity of the ratio R to the axial strange-quark form factor $F_A^s(0)$. First, comparing the curves of Fig. 2, which shows R vs Q^2 at $E_\nu=500$ MeV, with $F_A^s(0)=+0.1$ and $+0.2$, we see that at the larger Q^2 (backward angles), even very crude measurements of R are sufficient to observe a nonzero value of $F_A^s(0)$. The value of R is near its maximum of 1 in both cases. Changing the sign of $F_A^s(0)$ would result in a sign flip of R. When R is near its maximum, at backward angles, it is difficult to distinguish between the values of $F_A^s(0)=0.1$ and 0.2. To do this, one would need to go to more intermediate angles and Q^2. For example, at the same energy, with $Q^2=0.4$ GeV^2 ($\theta=90°$), Fig. 2 shows that a measurement of cross sections with errors around 10–20% would be roughly sufficient to distinguish $F_A^s(0)=0.1$ from $F_A^s(0)=0.2$.

In Fig. 7 the sensitivity to $F_A^s(0)$ is shown directly for fixed $\theta=180°$. We plot R as a function of $F_A^s(0)$ for three different incident energies. The nonlinearity is again quite apparent. For $F_A^s(0)\approx 0.1$, R has a broad maximum at moderate energies. Thus, as observed above, R here serves as a strong signal for the presence, and sign,

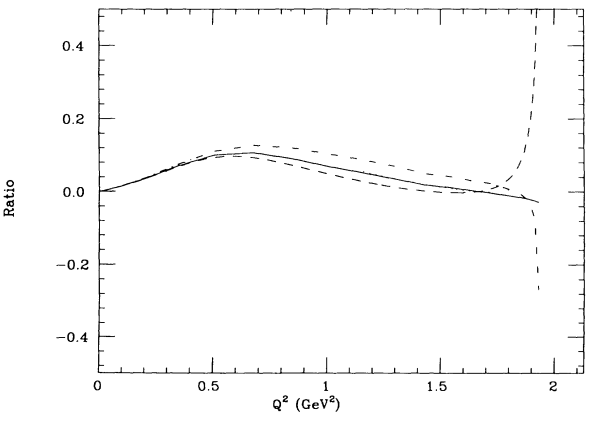

FIG. 4. Same as Fig. 3 for $F_A^s(0)=0.1$ at $E_\nu=1$ GeV for both Paris and Bonn potentials. Method B is shown dashed for the Paris and dotted for the Bonn potential; method C is shown solid for the Paris and dot-dashed for the Bonn potential.

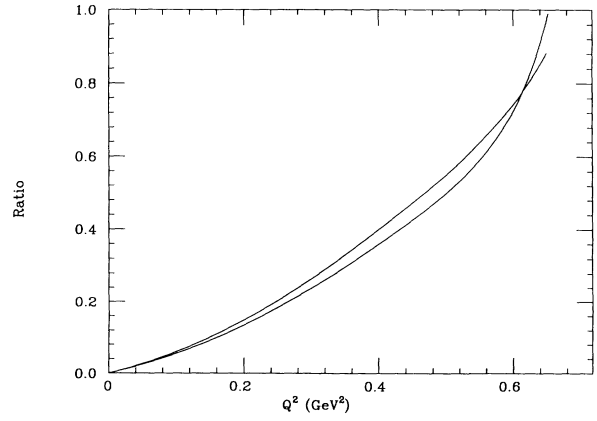

FIG. 6. R as a function Q^2. The curves shown bound the use of the Paris, Bonn, and Reid potentials and variations of the mass M_A in the axial form factor from 0.996 to 1.065 GeV/c^2.

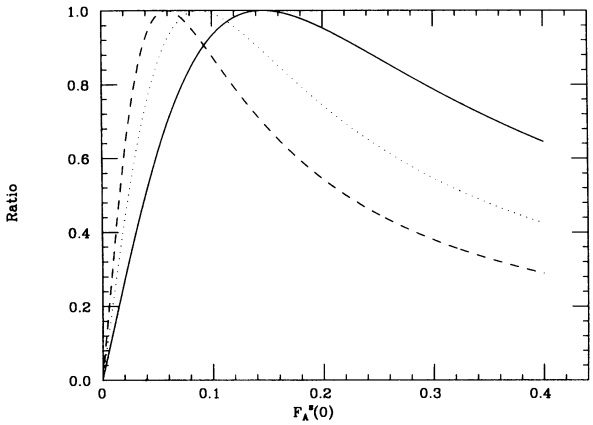

FIG. 7. R as a function $F_A^s(0)$ for backward (180°) ν and $\bar{\nu}$ scattering at $E_\nu=150$ (dashed), 250 (dotted), and 500 MeV (solid).

of a nonzero axial isoscalar form factor due to strange quarks. It is moderately insensitive to the specific value of $F_A^s(0)$. At smaller angles, the curves are "stretched out," and become more sensitive to the value of $F_A^s(0)$, at the cost of needing to measure a smaller R.

As discussed earlier, it is possible that strange quarks modify the weak vector form factors as well. In particular, an s-quark contribution to the nucleon's magnetic form factor is currently largely unconstrained by experiment. It is the object of a proposed experiment at BATES [7,9]. Such a contribution enters the ratio R by modifying the deuteron weak magnetic form factor, which interferes with G_A. In fact, the effects on R are similar to those of variations in the size of the axial isoscalar form factor, and thus one cannot easily extract $F_A^s(0)$ without further measurements. This is demonstrated in Fig. 8 where we show R vs Q^2 at 500 MeV, with $F_A^s(0)=0.2$, but allowing $F_M^s(0)$ to be 0, $+0.2$, or -0.2. Because there is already a finite, nonstrange, isoscalar magnetic form factor, R is not symmetric with respect to the sign of this quantity. The spread in Fig. 8 is roughly comparable to the spread caused by

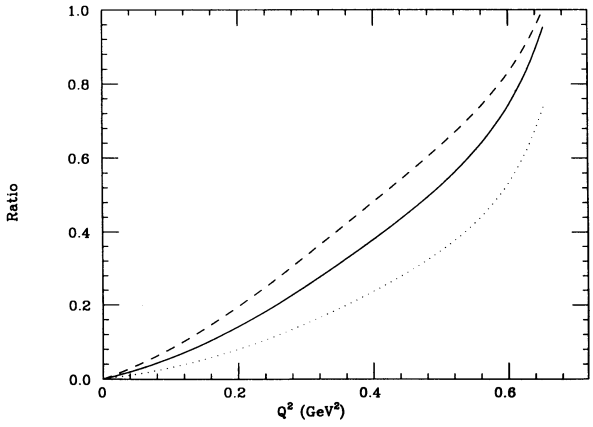

FIG. 8. R as a function of Q^2 at $E_\nu=500$ MeV for $F_A^s(0)=0.2$ and for $F_M^s(0)=0$ (solid), 0.2 (dashed), and -0.2 (dotted).

$F_A^s(0)\approx 0.2\pm 0.1$.

Such a nonzero vector s-quark matrix element would be very interesting in its own right, but some means is required to separate the effects of F_A^s from F_M^s. As mentioned, parity violation in lepton-hydrogen or lepton-deuteron scattering are possibilities. Another possibility, involving only neutrino (or $\bar{\nu}$) scattering, is to measure the $Q^2\to 0$ absolute cross section. This depends directly on $F_A^s(0)^2$, whereas the contributions from $F_M^s(0)$ and $F_E^*(0)$ to the forward cross section are both explicitly suppressed by factors of Q^2/M^2. For small Q^2 and θ, the ν (or $\bar{\nu}$) elastic differential cross section is given roughly by

$$\frac{d\sigma_{\nu(\bar{\nu})d}}{d\Omega}\approx\frac{G_F E_\nu^2}{2\pi^2}\left[(-2\sin^2\theta_W)^2+\frac{2}{3}F_A^2\right]+\mathcal{O}(Q^2)\ . \tag{46}$$

Experimentally, however, it is difficult to measure absolute normalizations of neutrino beams. Note that to get $|\delta F_A^{\rm IS}|\lesssim 0.15$ requires a neutrino cross section with less than 10% total uncertainty. Also, small Q^2 means the recoiling deuteron is difficult to detect. Thus, the R ratio (where overall normalization, at least, cancels) may be the best one can do with ν-d elastic scattering to detect strangeness form factors.

What is the best energy range of average neutrino energy at which to carry out these experiments? Figures 1–8 make it clear that there are various tradeoffs. A large Q^2 affords one an easier opportunity to detect the recoiling deuteron nucleus, but the cross section falls rapidly due to the deuteron body form factors. Furthermore, it is necessary to stay away from the zeros of these form factors. If one arbitrarily sets a criterion that the differential cross section $d\sigma/dQ^2$ should exceed some minimum, an upper bound on θ for any given beam energy is implied. This is simply because $d\sigma/dQ^2$ drops monotonically with $Q^2(\theta)$ for fixed E_ν. Similarly, requiring R to exceed some minimum value (which will be based on the experimental error estimates) generally implies a lower bound on θ given E_ν, because R tends to rise with $Q^2(\theta)$.

We demonstrate such kinematic bounds in Fig. 9, with $d\sigma/dQ^2\geq 10^{-41}$ cm^2/GeV^2 and $R\geq 0.25$ chosen for explicitness. There is clearly an allowed "window" of beam energies (under $\approx$400 MeV here) and scattering angles. As $d\sigma/dQ^2_{\rm min}$ is lowered, the upper-bound curve rises, opening the window. This is seen in Fig. 9 from the dashed curve, which shows the upper bound if the minimum measurable cross section is 10 times smaller than that assumed for the solid curve.

Similarly, as $R_{\rm min}$ is raised, the lower-bound curve rises, closing the window. Smaller values of $F_A^s(0)$ also raise the lower bound, but not significantly, especially at lower energies. This figure is intended only as a crude demonstration, as experimental constraints and correlations between $R_{\rm min}$ and $d\sigma/dQ^2_{\rm min}$ would have to be carefully considered to set up optimal kinematics for a real experiment.

In conclusion, we have shown that neutrino and antineutrino scattering cross sections on isospin-0, spin-1

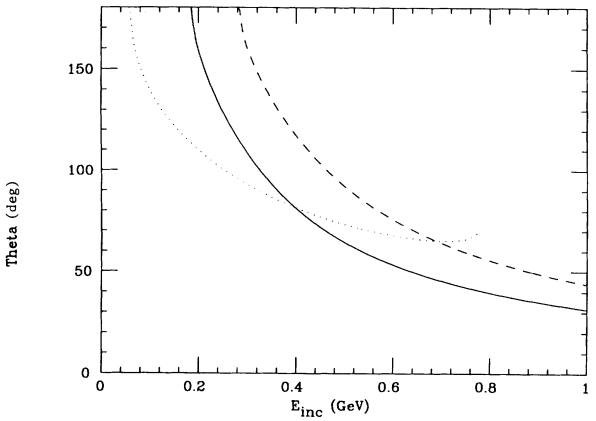

FIG. 9. Region of allowed kinematics, θ vs E_ν (see text). The upper-bound curves are obtained from the arbitrary constraints $d\sigma/dQ^2 \geq 10^{-41}$ cm^2/GeV^2 (solid) and $d\sigma/dQ^2 \geq 10^{-42}$ cm^2/GeV^2 (dashed). A lower-bound curve (dotted) is given by the constraint $R \geq 0.25$. All curves assume Paris wave functions and $F_A^s(0)=0.2$.

targets, particularly deuterium, can be used to measure strangeness matrix elements in the nucleon. We suggest the measurement of R, the ratio of the difference of ν and $\bar{\nu}$ scattering cross sections to the sum [Eq. (3)], as a means to extract information on the axial isoscalar nucleon form factor $F_A^{\rm IS}(q^2)$. This form factor in turn can be related to the strangeness axial-vector matrix element in the nucleon, F_A^s [Eq. (9)]. The ratio R vanishes if the isoscalar axial-vector matrix element is zero. When R is small, it is approximately directly proportional to $F_A^s(0)$. When R approaches unity, it remains sensitive to (but is no longer directly proportional to) $F_A^s(0)$ due to its appearance in the denominator of the ratio. If the strangeness vector matrix element F_M^s is also nonvanishing, then a separation of F_A^s and F_M^s requires a measurement of neutrino and antineutrino cross sections over a range of kinematic conditions. We also discuss the "best" neutrino energy region for the proposed measurement; it appears that average neutrino energies below 500 MeV are appropriate.

ACKNOWLEDGMENTS

One of us (T.F.) would like to acknowledge the support from Fundação de Amparo à Pesquisa do Estado de São Paulo (FAPESP), Brazil. E.M.H. is grateful to A. Thomas for his hospitality at the University of Adelaide, where some of this work was carried out. This work was supported in part by the U.S. Department of Energy.

APPENDIX: HADRONIC RESPONSE FUNCTIONS IN TERMS OF THE REDUCED MATRIX ELEMENTS OF MULTIPOLE OPERATORS

We adopt a phase convention for Y_{lm} such that

$$Y_{lm}^* = (-1)^m Y_{l-m} \ , \tag{A1}$$

where Y_{lm} is a spherical harmonics. It is found that the response functions $R_{ss}, \ldots, R_{vv}$ are

$$R_{ss}(\sigma)=\sqrt{4\pi}\tilde{\sigma}\sum_{\lambda J_f}\sum_{JJ'}(-1)^{J_i+J_f+J+\sigma}\begin{Bmatrix} J_i & J' & J_f \\ J & J_i & \sigma \end{Bmatrix} F_{ss}(\lambda J_f;JJ'\sigma) \ , \tag{A2}$$

$$R_{sv}^{\pm}(\sigma\rho)=\sqrt{4\pi}\tilde{\sigma}\sum_{\lambda J_f}\sum_{JJ'}(-1)^{J_i+J_f+J+\sigma}\begin{Bmatrix} J_i & J' & J_f \\ J & J_i & \sigma \end{Bmatrix} F_{sv}^{\pm}(\lambda J_f;JJ'\sigma\rho) \ , \tag{A3}$$

$$R_{vv}(\sigma\rho\tau)=\sqrt{4\pi}\tilde{\sigma}\sum_{\lambda J_f}\sum_{JJ'}(-1)^{J_i+J_f+J+\sigma}\begin{Bmatrix} J_i & J' & J_f \\ J & J_i & \sigma \end{Bmatrix} F_{vv}(\lambda J_f;JJ'\sigma\rho\tau) \ , \tag{A4}$$

with

$$F_{ss}(\lambda J_f;JJ'\sigma)=(i)^{J-J'}(-1)^J\frac{\langle\sigma\|Y_{J'}\|J\rangle}{\tilde{\sigma}}\mathcal{C}_J(\lambda J_f)\mathcal{C}_{J'}^*(\lambda J_f) \ , \tag{A5}$$

$$F_{sv}^{\pm}(\lambda J_f;JJ'\sigma\rho)=(i)^{J-J'}f_{sv}(\lambda J_f;JJ'\sigma\rho)\pm f_{vs}(\lambda J_f;JJ'\sigma\rho) \ , \tag{A6}$$

$$F_{vv}(\lambda J_f;JJ'\sigma\rho\tau)=(i)^{J-J'}(-1)^\rho\tilde{J}^2\tilde{J}'^2\tilde{\tau}\sum_{ll'}(-1)^{l+1}\langle\rho\|Y_{l'}\|l\rangle\begin{Bmatrix} 1 & l' & J' \\ 1 & l & J \\ \tau & \rho & \sigma \end{Bmatrix} a_l^J(\lambda J_f)a_{l'}^{J'}(\lambda J_f) \ , \tag{A7}$$

and

$$f_{sv}(\lambda J_f;JJ'\sigma\rho)=(-1)^\sigma\tilde{J}'^2\sum_l\langle\rho\|Y_J\|l\rangle\begin{Bmatrix} J & l & \rho \\ 1 & \sigma & J' \end{Bmatrix}\mathcal{C}_J(\lambda J_f)a_l^{J'*}(\lambda J_f) \ , \tag{A8}$$

$$f_{vs}(\lambda J_f;JJ'\sigma\rho)=(-1)^{J+1}\tilde{J}^2\sum_l(-1)^l\langle\rho\|Y_{J'}\|l\rangle\begin{Bmatrix} J' & l & \rho \\ 1 & \sigma & J \end{Bmatrix}a_l^J(\lambda J_f)\mathcal{C}_{J'}^*(\lambda J_f) \ , \tag{A9}$$

and

$$a^J_{J-1}(\lambda J_f)=(-1)^J\frac{1}{2J+1}[\sqrt{J+1}\,\mathcal{E}_J(\lambda J_f) + \sqrt{J}\,\mathcal{L}_J(\lambda J_f)]\ , \tag{A10}$$

$$a^J_J(\lambda J_f)=(-1)^J\frac{1}{\sqrt{2J+1}}\mathcal{M}_J(\lambda J_f)\ , \tag{A11}$$

$$a^J_{J+1}(\lambda J_f)=(-1)^J\frac{1}{2J+1}[\sqrt{J}\,\mathcal{E}_J(\lambda J_f) - \sqrt{J+1}\mathcal{L}_J(\lambda J_f)]\ , \tag{A12}$$

where λ enumerate different final states of the NN system with the same total and angular momentum, which is defined in Ref. [11]. The quantity $\tilde{L}$ is defined as

$$\tilde{L}\equiv\sqrt{2L+1}\ . \tag{A13}$$

The reduced matrix elements $\mathcal{C}_J$, $\mathcal{L}_J$, $\mathcal{E}_J$, and $\mathcal{M}_J$ of the hadronic charged weak currents can be decomposed into

$$\mathcal{C}_J(\lambda J_f)=C_J(\lambda J_f)+C^5_J(\lambda J_f)\ , \tag{A14}$$

$$\mathcal{L}_J(\lambda J_f)=L_J(\lambda J_f)+L^5_J(\lambda J_f)\ , \tag{A15}$$

$$\mathcal{E}_J(\lambda J_f)=E_J(\lambda J_f)+E^5_J(\lambda J_f)\ , \tag{A16}$$

$$\mathcal{M}_J(\lambda J_f)=M_J(\lambda J_f)+M^5_J(\lambda J_f)\ , \tag{A17}$$

where superscript "5" indicates that the corresponding matrix element originates from the axial-vector current and the remainder from the vector current.

The response function R_{ss} is a linear combination of bilinear products of the density operator J^0. The response function $R^{\pm}_{sv}$ is a linear combination of the symmetric/antisymmetric (with respect to the Lorentz indices μ) part of the bilinear products of the density operator J^0 and the current operator $\mathbf{J}$. The response function R_{vv} is a linear combination of bilinear products of the current operators $\mathbf{J}$. The rank of the response functions is determined by the value of $\sigma=0,1,\ldots,2J_i$, which corresponds to the degree of the irreducible polarization tensor of the hadronic system (initial, final, or both). For example, the $\sigma=0$ response functions are those which contribute to reactions where the hadronic system is unpolarized; the $\sigma=1$ response functions can be accessed only by polarization of the initial or final (or both) hadronic system; the $\sigma=2$ response functions occur in experiments where the hadronic system contains alignment. A property of the irreducible response functions is that they are of order $(Rq)^\rho$ (note that ρ coincides with σ for R_{ss}) in the leading q expansion, where R is a typical size of the nuclear system. This property can be used to analyze the order of magnitude of each of the irreducible response functions at low energies.

[1] T. P. Cheng and R. F. Dashen, Phys. Rev. Lett. **26**, 594 (1971); Phys. Rev. D **13**, 216 (1976); T. P. Cheng, *ibid.* **13**, 2161 (1973); C. A. Dominguez and P. Langacker, *ibid.* **24**, 190 (1981); J. Donoghue, Annu. Rev. Nucl. Part. Sci. **39**, 1 (1989).

[2] J. Ashman *et al.*, Phys. Lett. B **206**, 364 (1988); Nucl. Phys. **B328**, 1 (1989).

[3] M. A. Nowak, J. J. M. Verbaarshot, and I. Zahed, Phys. Lett. B **217**, 157 (1989); H. Fritzch, *ibid.* **229**, 122 (1989); Mod. Phys. Lett. A **5**, 1815 (1990); R. Anselmino and M. D. Scadron, Phys. Lett. B **229**, 117 (1989).

[4] J. Stern and G. Cle'ment, Phys. Lett. B **231**, 471 (1989); V. Bernard and U. Meissner, *ibid.* **216**, 392 (1989); **223**, 439 (1989); R. L. Jaffe and A. Manohar, Nucl. Phys. **B337**, 509 (1990); H. Lipkin, Phys. Lett. B **256**, 284 (1991).

[5] J. Ellis and M. Karliner, Phys. Lett. B **213**, 73 (1988); J. Ellis, M. Karliner, and C. Sachrajda, *ibid.* **231**, 497 (1989).

[6] R. L. Jaffe and A. Manohar, Nucl. Phys. **B337**, 509 (1990).

[7] R. Decker and Th. Leize, Phys. Lett. B **246**, 233 (1990); Fayyazuddin and Riazuddin, Phys. Rev. D **42**, 794 (1990); R. D. McKeown, Phys. Lett. B **219**, 140 (1989); E. J. Beise and R. D. McKeown, Comments Nucl. Part. Phys. **20**, 105 (1991); J. Napolitano, Phys. Rev. C **43**, 1473 (1991).

[8] E. M. Henley, G. Krein, S. J. Pollock, and A. G. Williams, Phys. Lett. B **269**, 31 (1991).

[9] D. H. Beck, Phys. Rev. D **39**, 3248 (1989).

[10] See, e.g., J. D. Walecka, in *Muon Physics,* edited by V. W. Hughes and C. S. Wu (Academic, New York, 1975), Vol. 2, p. 113.

[11] S. Ying, E. M. Henley, and G. A. Miller, Phys. Rev. C **38**, 1584 (1988); S. Ying, W. C. Haxton, and E. M. Henley, *ibid.* **40**, 3211 (1989); S. Ying, Ph.D. thesis, University of Washington (unpublished).

[12] S. J. Pollock, Phys. Rev. D **42**, 3010 (1990).

[13] See, e.g., T. Frederico, E. M. Henley, and G. A. Miller, Nucl. Phys. **A533**, 617 (1991).

[14] L. L. Frankfurt and M. I. Strikman, Nucl. Phys. **B148**, 107 (1979); Phys. Rep. **76**, 215 (1981); B. L. G. Bakker, L. A. Kondratyuk, and M. V. Terent'ev, Nucl. Phys. **B158**, 497 (1979); L. A. Kontratyuk and M. V. Terent'ev, Yad. Fiz. **31**, 1087 (1980) [Sov. J. Nucl. Phys. **31**, 561 (1980)].

[15] W.-Y. P. Hwang and E. M. Henley, Ann. Phys. (N.Y.) **129**, 47 (1980).

[16] F. Gross, Phys. Rev. **136**, B140 (1964); M. Gourdin, Nuovo Cimento **28**, 533 (1963); J. E. Elias *et al.*, Phys. Rev. **177**, 2075 (1969); R. G. Arnold, C. E. Carlson, and F. Gross, Phys. Rev. C **21**, 1426 (1980).

[17] S. J. Pollock, Ph.D. thesis, Stanford University, 1987 (unpublished).

[18] R. Reid, Ann. Phys. (N.Y.) **50**, 411 (1968); R. Machleidt, K. Holinde, and Ch. Elster, Phys. Rep. **149**, 1 (1987); M. Lacombe *et al.*, Phys. Lett. **101B**, 139 (1981).

[19] P. L. Chung, F. Coester, B. D. Keister, and W. N. Polyzou, Phys. Rev. C **37**, 2000 (1988).

[20] I. L. Grach and L. A. Kontratyuk, Yad. Fiz. **39**, 316 (1984) [Sov. J. Nucl. Phys. **39**, 198 (1984)].

[21] J. M. Namyslowski, Prog. Part. Nucl. Phys. **14**, 49 (1985).

[22] F. Coester and A. Ostebee, Phys. Rev. C **11**, 1836 (1975).

[23] L. L. Frankfurt, I. L. Grach, L. A. Kondratyuk, and M. Strikman, Phys. Rev. Lett. **62**, 387 (1989).

[24] L. A. Ahrens *et al.*, Phys. Rev. D **35**, 785 (1987).

[25] M. Gari and W. Krumpelmann, Z. Phys. A **332**, 689 (1985).